UDK 620.18:544.3:67.014:669.131.6:661.666.2
Original scientific article/Izvirni znanstveni članek

ISSN 1580-2949
MTAEC9, 55(4)533(2021)

ANALYSIS AND THERMODYNAMIC STABILITY OF NUCLEI IN SPHEROIDAL GRAPHITE IN Fe–C–Si ALLOYS

ANALIZA IN TERMODINAMSKA STABILNOST KALI V KROGLASTEM GRAFITU PRI Fe-C-Si ZLITINAH

Marica Prijanovič Tonkovič[1], Primož Mrvar[2], Maja Vončina[2], Črtomir Donik[3], Matjaž Godec[3], Mitja Petrič[2]*

[1]Short-cycle Higher Vocational College – Novo mesto, Slovenia
[2]University of Ljubljana, Faculty of Natural Sciences and Engineering, Department of Materials and Metallurgy, Ljubljana, Slovenia
[3]Institute of Metals and Technology, Ljubljana, Slovenia

Prejem rokopisa – received: 2021-03-01; sprejem za objavo – accepted for publication: 2021-04-09

doi:10.17222/mit.2021.063

The paper describes the graphite nuclei constitution for spheroidal graphite cast iron melted in a cupola furnace, which is treated by the addition of magnesium and inoculated with a barium-based inoculant. Two samples of spheroidal cast iron were analysed, differing only in tin content. Field-emission scanning electron microscopy (FE -SEM) with energy-dispersive X-ray spectroscopy (EDS) was used to analyse the nuclei. The thermodynamic calculation of the phase equilibria and the associated free formation energies of the alloys were calculated and compared with metallographic observations. It was found that the nuclei in the spheroidal graphite are different in shape and composition. Spherical and rectangular ones were found, and in many cases the porosity was present at the nuclei. The nuclei consisted of different compounds such as (Mg,Ca)S, MgO, (Mg,Al,Si)N. The amount of Sn only affected the pearlite content, and there were no Ba and rare earths present in the nuclei.

Keywords: spheroidal graphite cast iron, graphite, nuclei, inclusions

V raziskavi smo ugotavljali sestavo kali v grafitnih kroglah sive litine s kroglastim grafitom, ki je bila proizvedena v kupolni peči in je bila po nodulaciji z dodatkom magnezija (Mg) cepljena z cepivom na osnovi barija (Ba). Za raziskavo smo pripravili dva vzorca, ki sta se razlikovala v dodatku kositra. Za analizo kali je bil uporabljen vrstični elektronski mikroskop na poljsko emisijo (FE-SEM), opremljen z energijsko disperzijsko rentgensko spektroskopijo (EDS). Termodinamični izračun faznih ravnotežij omenjenih zlitin je bil izračunan in primerjan z metalografskimi opazovanji. Ugotovljeno je bilo, da so kali v grafitnih kroglah različne po obliki in sestavi. Najdeni so bili sferični in pravokotni vključki, v veliko primerih pa je bila ob kaleh prisotna poroznost. Jedra grafitnih krogel so sestavljale različne spojine, kot so (Mg, Ca)S, MgO, (Mg,Al,Si)N. Količina kositra je vplivala le na vsebnost perlita, v kaleh pa ni bilo barija in redkih zemelj (RE).

Ključne besede: siva litina s kroglastim grafitom, grafit, kali, vključki

1 INTRODUCTION

Graphite in cast irons can occur in various shapes. The most desired shapes are lamellar, spheroidal and vermicular shapes, which give different mechanical and other useful properties to the alloys.[1] The shape, size and distribution of the graphite result from the chemical composition of the melt and from the cooling conditions during solidification. The spheroidal shape of graphite is usually achieved by deoxidation and desulphurization of the melt, which in most cases is achieved by additions of magnesium (Mg), which enables the growth not only in the a-direction but also in the c-direction.[1,2] The distribution and size of the nodules in spheroidal graphite cast iron are always desired as homogeneous and fine, which is achieved by inoculation. The inoculation process ensures the formation of particles or inclusions that can act as nuclei for graphite growth. Usually, the inoculation agents or so-called inoculants are based on FeSi master alloys with added elements such as barium (Ba), calcium (Ca), strontium (Sr), zirconium (Zr) or elements of the rare earths (REs).[1–5]

There are many graphite nucleation theories that have been presented over the decades and collected in papers.[6,7] There are theories such as the gas bubble theory of Nieuwland and Karsay, the carbide theory of Boyles, the salt-like carbide theory of Lux, the silicon carbide theory of Wang and Fredriksson, the sulphide/oxide theory and later the silicate theory of Skaland.

However, it has been found that the nuclei consist of oxides, sulphides, nitrides, carbides, etc.[6,8] In many cases they were found to be complex phases. Y. Igarashi[9] and H. Nakae[10] reported on MgO and/or MgS as the nuclei for graphite, and occasionally the nitrides ((Mg,Si,Al)N) are attached too. They suggest that rounded MgS acts as a nucleus for graphite. T. Skaland et al.[6,11] showed that the nuclei consist of primary and secondary products of magnesium treatment. In this case, MgS and CaS represent the core of a nuclei surrounded by a layer of $MgO \times SiO_2$ or $2MgO \times SiO_2$. When inoculated with ferrosilicon based on Ca, Sr, Ba and Al-based ferrosilicon the hexagonal silicate phases $XO \times Al_2O_3 \times 2SiO_2$ can be formed on the surface of the oxide core.

*Corresponding author's e-mail:
mitja.petric@omm.ntf.uni-lj.si (Mitja Petrič)

D. M. Stefanescu et al.[12] and G. Alonso et al.[7] used cast-iron melts with different Ti contents and reported about Ti-carbides (TiC) and Ti-carbonitrides (TiCN) found in the centres of the graphite nodules, besides the above-listed phases. They also report on RE oxides and sulphides present in the centres of the nodules. When using Ba-based inoculants, they do not report Ba-based oxides and sulphides in the cores of the nodules.

The aim of the present work is to compare and understand the nature of the graphite nuclei in commercial cast-iron melt samples solidified under normal industrial conditions.

2 EXPERIMENTAL

2.1 Sample preparation

We have produced two samples of spheroidal graphite cast iron in an industrial environment. The melt was produced in a coke-fired cold blast cupola furnace by melting spheroidal graphite cast iron returns and steel scrap. The melt was desulphurised with calcium carbide and transported into the channel-type induction holding furnace. The melt for the samples was Mg-treated and inoculated in a ladle using the sandwich process, whereby the magnesium master alloy (1 *w*/%) as a nodulariser was covered with steel scrap and poured over by the melt. A Ba-based inoculant (0.2 *w*/%) was added to the melt during the overpouring process. The chemical compositions of nodularising agent and inoculant are given in **Table 1**. The REs are mainly represented by cerium (Ce) and lanthanum (La). Before casting the samples, the two different amounts of tin (Sn) were added to the melts to obtain different amounts of pearlite in spheroidal graphite cast irons with different tensile strength and to investigate whether Sn has some influence on the mechanism of graphite nucleation. The chemical composition of the melt prior to treatment (base) and of two cast samples are given in **Table 2**.

The samples were poured into a measuring cell produced by a Croning process and had the shape of a rod with a square cross-section of 320 mm^2 and a length of 210 mm. The measuring cell is described in detail in earlier publications.[13,14] The estimated cooling rate was 10 K/s, which gives a solidification time of about 100 s.

2.2 Characterization

Metallographic samples were taken from the casting next to the sprue. First, the samples were metallographically prepared by grinding and polishing and observed with an Olympus BX61 optical microscope. Graphite analysis and the portions of ferrite and pearlite were determined with an image-analysis system with an integrated EN ISO 945 standard. A scanning electron microscope (SEM) JEOL JSM 5610, equipped with an energy-dispersive X-ray spectroscopy detector (EDS) was also used. It was found that classic grinding and polishing damaged the samples too much for good SEM images, while some graphite nodules were extracted from the sample, so that the EDS analyses also yielded incorrect results. In addition, the metallographic samples were again prepared by cross-section polishing with the JEOL cross-section polisher, whereby the surface is cut by Ar^+ ions, so that the observed surface is undamaged and uncontaminated. The prepared samples were then observed and analysed with a field-emission scanning electron microscope (FE -SEM) JEOL JSM-6500F, which was also equipped with an EDS detector. To determine the main elements, present in the inclusions, spectra, mapping and line scans were performed and presented.

2.3 Thermodynamic calculation of equilibrium

According to the chemical composition of the cast samples, a thermodynamic equilibrium of the phases and the free Gibbs energies of formation for the present phases were calculated with the Thermo-Calc 2020a software using the TCFE8 database. Since it is known that nuclei also consist of elements that are not specified in the composition of the melt (**Table 2**), nitrogen (0.007 *w*/%), calcium (0.001 *w*/%) and oxygen (0.005 *w*/%) were included in the calculation according to literature sources that give approximate quantities of the listed elements.[15,16] Elements such as Cr, V and Ni were not included in the calculation because they are not known to be potential elements to form nuclei. Barium

Table 1: Chemical compositions of nodularising agent and inoculation agent

	Chemical composition (*w*/%)						
	Fe	Si	Ca	Al	Ba	Mg	RE
Nodulariser	Rest	44– 48	0.8–1.2	0.4–1.0	–	5.5–6.2	0.8–1.2
Inoculant	Rest	64–70	1.0–2.0	0.8–1.5	2.0–3.0	–	–

Table 2: Chemical compositions of investigated samples

Sample	Chemical composition (*w*/%)												CE
	C	Si	Mn	S	Cr	Cu	P	Mg	Ni	Ti	Sn	Al	
Base	3.95	1.82	0.259	0.048	0.04	0.026	0.031	0.05	0.017	0.009	0.021	0.00	4,59
1	3.73	2.56	0.294	0.009	0.039	0.028	0.025	0.038	0.019	0.008	0.031	0.003	4.55
2	3.70	2.54	0.324	0.008	0.039	0.029	0.026	0.036	0.019	0.008	0.053	0.006	4.58

as an inoculation agent was not considered because it was not supported by the software databases. Even a combination of the TCFE8 and SSOL5 database was considered, but no promising results were achieved. The results obtained give us an insight into the stability of the different phases in temperature ranges above the liquidus temperature and in the solid.

3 RESULTS

3.1 Metallographic investigation

In the first step of the metallographic investigation, the samples were prepared with classic metallographic preparation by grinding and polishing. The samples prepared in this way were examined with optical and SEM microscopes. **Figure 1** is an optical micrograph of the examined sample. It can be seen that the microstructure is very similar in terms of graphite. The graphite size in both cases is from class 6, the shape is from class VI, the amount of graphite is 9.8 area percent and the nodularity is 0.64 in sample 1 and 0.72 in sample 2. There is an obvious difference between the ferrite and pearlite fractions, with 62 area percent pearlite in sample 1 and 73 area percent pearlite in sample 2, which is the result of a higher amount of Sn in the chemical composition.

With improved sample preparation and using the FE-SEM microscope, the results were more promising because the particles located in the centres of the graphite spheres were not extracted during the preparation. In both samples approximately 50 particles were examined. We did not find any differences in the two samples examined, where the type of particles found as nuclei was the same. From this it was concluded that Sn has no influence on nucleation. The following the illustrations show representative particles from both samples.

Figure 2 shows a graphite nodule with a particle in the middle. It appears as if the particle consists of two spheres connected to each other, but the analysis shows that it is one phase. EDS analysis and mapping show that it consists of Mg, Ca and S. Fe and C are most likely the influence of the EDS analysis, where the background of

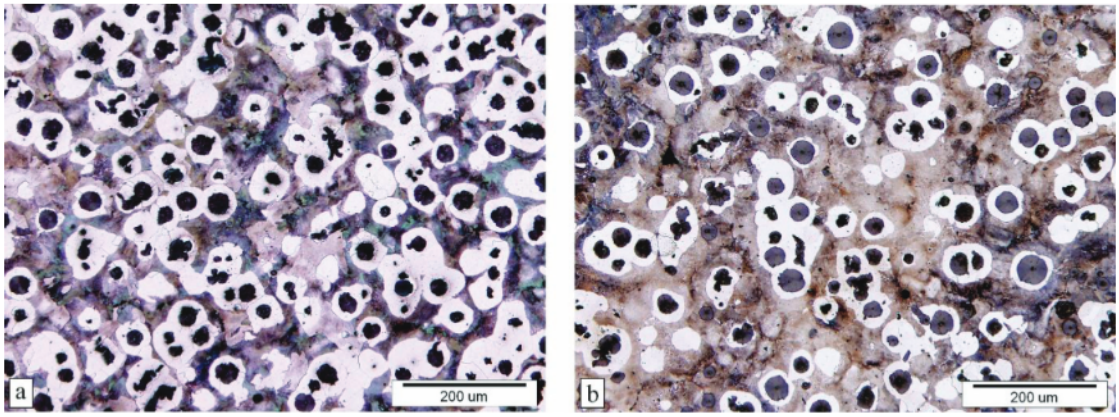

Figure 1: Optical micrograph of investigated samples: a) sample 1, b) sample 2

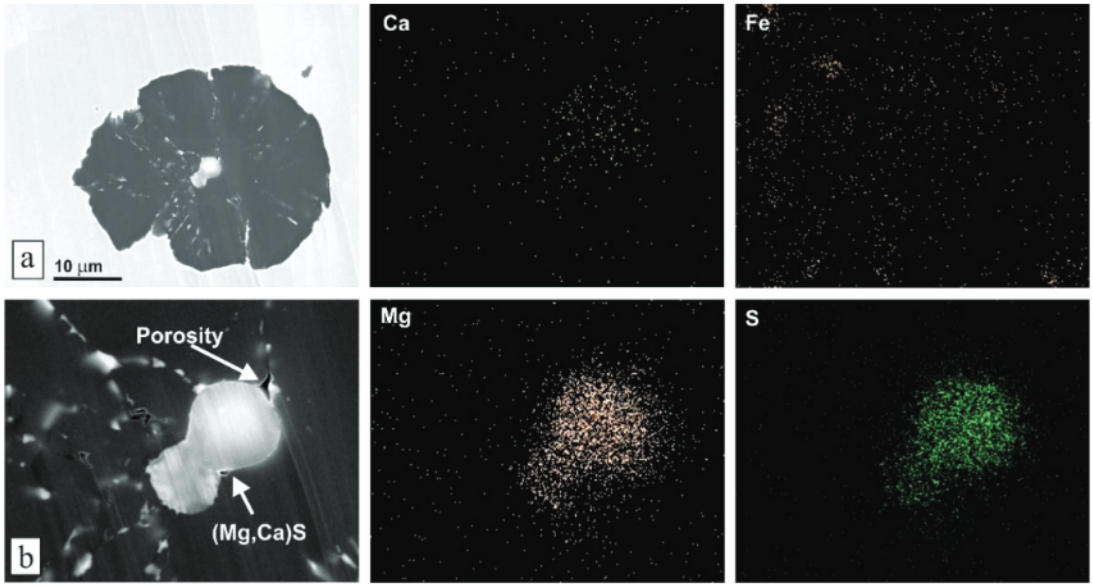

Figure 2: a) Graphite nodule with a (Mg,Ca)S particle in the centre, b) enlarged particle with corresponding mapping EDS analysis (sample 2)

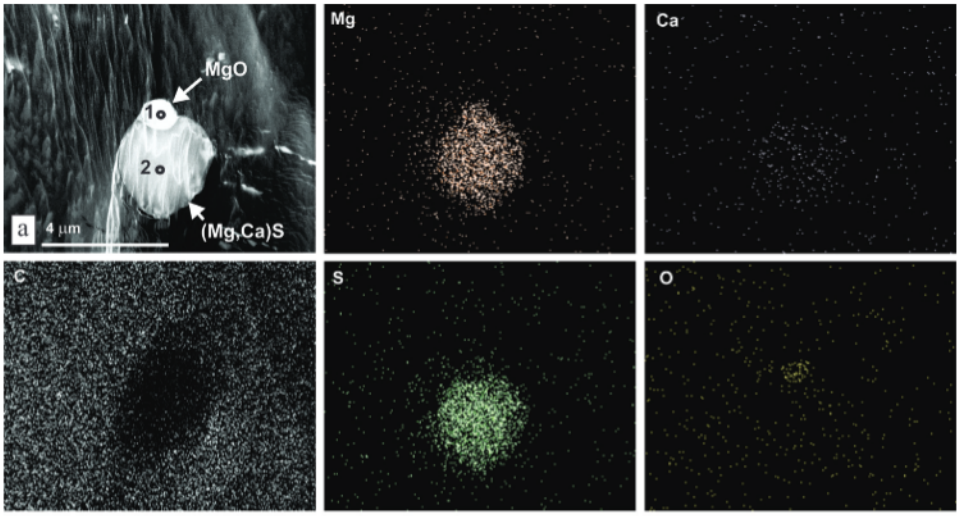

b

x/%	C	O	Mg	S	Ca	Fe
Spectr. 1	40.80	29.32	22.83	3.14	0.00	3.91
Spectr. 2	59.59	0.00	14.66	21.04	1.68	3.04

Figure 3: a) Particle in the graphite centre with mapping EDS analysis; b) EDS analyses of two noted spectra (sample 2)

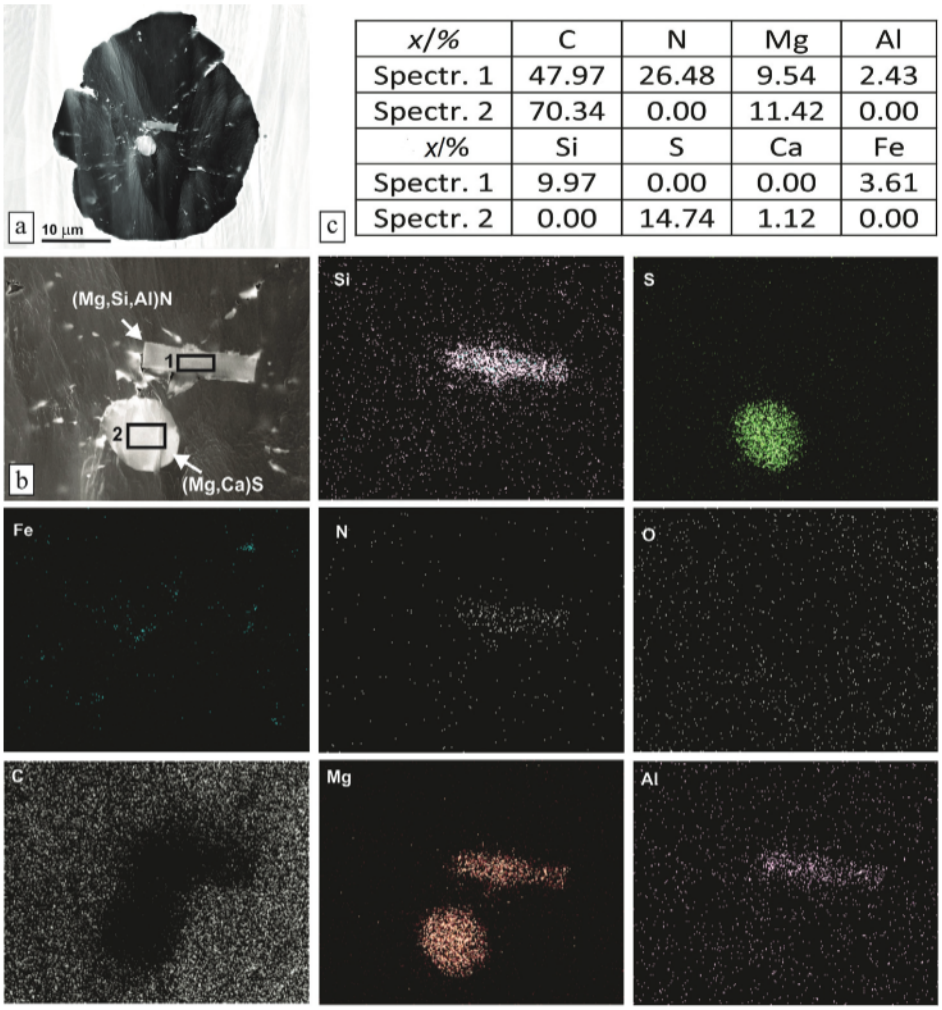

c

x/%	C	N	Mg	Al
Spectr. 1	47.97	26.48	9.54	2.43
Spectr. 2	70.34	0.00	11.42	0.00
x/%	Si	S	Ca	Fe
Spectr. 1	9.97	0.00	0.00	3.61
Spectr. 2	0.00	14.74	1.12	0.00

Figure 4: Analysis of graphite nucleus: a) graphite nodule with particle in the centre; b) corresponding analyses of particle; c) EDS analyses of two marked spots (sample 2)

the sample is analysed and confirmed by mapping, as there is no increased amount of Fe and C in the particle. The amount of Mg is about ten times greater than the amount of Ca.

In this case and in many cases that are also described below, porosity is present next to the nucleus. The graphite growth seems to be conical or columnar, with iron between the columns or cones, as shown in **Figure 3** with white spots and lines in the graphite nodule.

Figure 3 shows another particle in the graphite nodule. The difference to the particle shown in **Figure 2** is that it consists of two different phases. The upper one is white and partially embedded by a greyish particle. Both are rounded or spherical. The EDS analysis is shown in **Figure 3b**, where the white part is MgO, where a small amount of S is present, and the greyish part is similar to the particles shown in **Figure 2**.

Particles that have the potential to act as nuclei were not always spherical, but some rectangular particles were found next to (Ca,Mg)S. In contrast to others, these rectangular ones were complex nitrides with Mg, Si and to a lesser extent with Al((Mg,Si,Al)N). Usually they were not found alone in the centres of graphite spheres, but in contrast to other reports[9,10] these were not in direct contact with other particles – in this case (Mg,Ca)S. **Figure 4** shows that the two particles are not connected, which means that the particles were present in the melt before graphite formation. It cannot be stated which particle is more suitable for graphite nucleation. SEM micrographs and EDS analyses of the particles mentioned are shown in **Figure 4**.

In a case shown in **Figure 5**, the structure of the complex particle is slightly different from the structure described above and reported by other authors. A particle contains Mg, O, a small amount of Ca and a rather high amount of S. It is not clear whether it is a single phase or a complex multiphase. From the mapping analysis and the line EDS analysis it can be determined that oxygen and sulphur are present in the same area, which is brighter on the SEM micrograph given in **Figure 5a**, and from this it cannot be concluded whether it is one phase, or several phases bound together. In the latter case, the particle could consist of MgO, next to which the phase composed of Mg, O and S is present (EDS analysis of spot 2 in **Figure 5b**). Both phases mentioned above are then embedded by (Mg,Ca)S, which is then partly surrounded by iron and the rest by graphite.

3.2 Free Gibbs energies

The free Gibbs energies of possible equilibrium phases were calculated for the alloys under investigation in the temperature ranges from liquid to solid. **Figure 6** shows the free Gibbs energies, and it can be seen that the most stable possible phase in a system is MgO, followed by complex sulphides ((Mg,Ca)S) and titanium and mag-

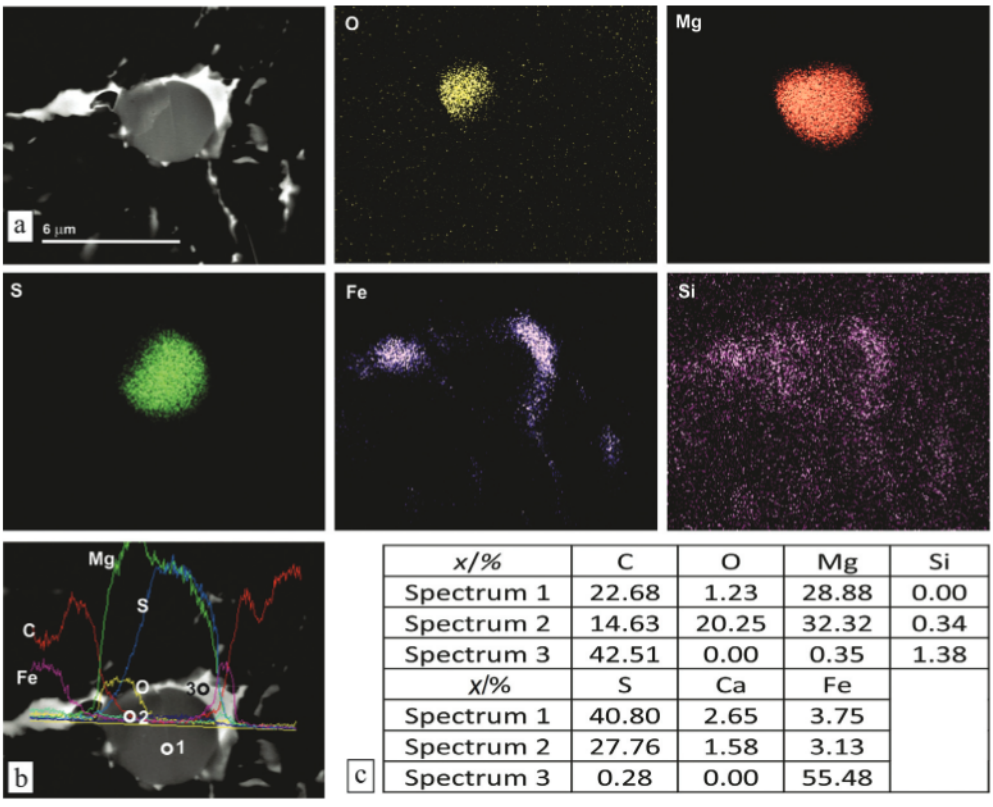

c

x/%	C	O	Mg	Si
Spectrum 1	22.68	1.23	28.88	0.00
Spectrum 2	14.63	20.25	32.32	0.34
Spectrum 3	42.51	0.00	0.35	1.38
x/%	S	Ca	Fe	
Spectrum 1	40.80	2.65	3.75	
Spectrum 2	27.76	1.58	3.13	
Spectrum 3	0.28	0.00	55.48	

Figure 5: a) Analysis of complex particle; b) line EDS analysis with marked spots of analysis; c) EDS analyses of three marked spots (sample 1)

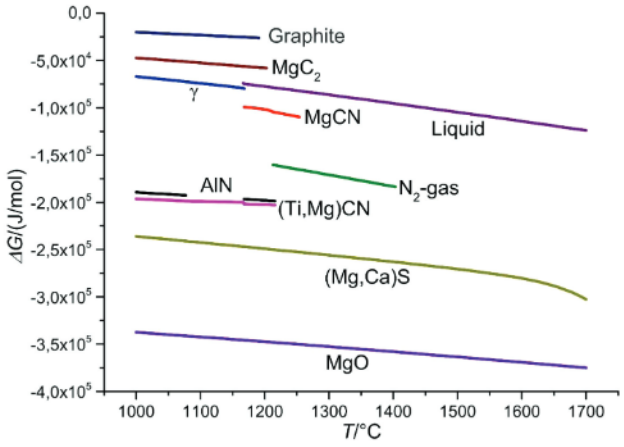

Figure 6: Free Gibs energy of formation for phases in investigated alloys

nesium carbonitrides ((Ti,Mg)CN). Aluminium nitride (AlN) and magnesium carbonitride (MgCN) as well as magnesium carbide (MgC_2) are also calculated as possible phases present. The free formation energies differ from those given in the literature,[7,9] probably because of the different calculation approach. In our case, a whole chemical composition of the melt was considered, where the activities of the individual elements are changed in the presence of other elements that influence the free energy of formation. No significant differences were observed in two samples analysed, which differ in Sn content which means that the Sn contents used in industrial alloys have little effect on the formed phases and the corresponding free formation energies.

According to the calculation of the thermodynamic equilibrium and the EDS analysis of the particles shown in **Figure 2**, it should be magnesium-calcium sulphide ((Mg,Ca)S), where the amount of S is 50 *x*/%. The thermodynamic equilibrium calculation shows that the amount of Mg in (Mg,Ca)S is about 45 *x*/% and the amount of Ca is about 5 *x*/%. These results are in good agreement with the EDS analysis, which shows that the amount of Mg is ten times greater than that of Ca. In most cases, the sulphides were found in the centres of the nodules, so from this point of view the sulphides are the main nuclei for graphite nucleation.

As can be seen from **Figure 6**, MgO has the lowest free energy of formation, i.e., it is most stable, and one could expect that MgO is initially formed in the melt. As shown in **Figure 3**, the MgO is embedded by (Ca,Mg)S, which is the next most stable phase from a thermodynamic point of view. The mechanism could be that MgO is a substrate for sulphide, which can then act as a nucleus for graphite.

From **Figure 4** it can be seen that complex nitrides are also present in the centres of the nodules. The results from the thermodynamic calculations also show an aluminium nitride (AlN) with a free formation energy just above (Ca,Mg)S. The reason for the discrepancy between the complex nitride (Mg,Si,Al)N and the AlN could be found in the equilibrium conditions for the calculation and non-equilibrium conditions for the experimental result, where it seems that complex nitrides can be formed. From the presented results we confirmed that the nitrides are present in the graphite nodules, and based on previous reports[9,10] the nitrides are also possible nuclei for graphite nucleation.

4 DISCUSSION

From all the results presented it can be seen that in most cases the sulphides are present in the nucleus in the form of (Mg,Ca)S. MgS was not found and was not predicted by calculating the free formation energies. To a lesser extent, MgO and nitrides were detected. Similar observations were made by Igarashi and Alonso.[7,9] They claim that the nucleation mechanism is such that MgO is first formed in combination with MgS and nitrides. According to our findings we have confirmed that the MgO is first formed and then surrounded by (Mg,Ca)S, which is also supported by the calculation of the free formation energies. However, nitrides were not in contact with the sulphide, so it is not clear which of them is formed first, but after the calculating the free energy of formation it should be later. Also, the frequency of appearance of the nitrides was the lowest from all the analysed particles. In Igarashi's work[9] it is also stated that the MgS could be liquid at the beginning of the graphite crystallisation, but in our case the thermodynamic equilibrium calculation showed that the solid (Mg,Ca)S and MgO are already formed in the melt at temperatures above 1700 °C.

In this work we could not confirm the nucleation mechanism of Skaland[6,11] because no such complex particles were found in our specimens. We also found no evidence of elements such as Ba and REs contained in the nodulariser and inoculant (**Table 1**). Other authors claim that they are not found because they are added in small amounts, but the content of these elements is similar to the Ca content in this example. The Ca enters the process through desulphurization and inoculation, and we can detect it. The Ba and RE have entered the system through the same processes, and the quantities should also be in the detectable range, but this is not the case. It is therefore not clear whether these elements are dissolved in a solid solution or whether they burn out during the process or produce other complex particles that have not been detected.

The theory of the nucleation mechanism of spheroidal graphite is not yet fully understood. Different authors report on the presence of different phases, and it seems that the process of melt treatment and the use of different nodularisers and inoculants can produce different results and therefore different mechanisms.

5 CONCLUSIONS

The aim of this study was to understand the nature of the particles that can act as nuclei for spheroidal graphite in cast iron under industrial solidification conditions. Two alloys with similar chemical compositions, except for tin, were analysed and no significant difference in the nuclei was found. From this it is concluded that tin only affects the perlite content and has no influence on the formation of the graphite nuclei.

Various nucleation theories assume that the nuclei consist of single-phase particles or that the particles are complex phases of sulphides, which in some cases are surrounded by complex oxides or nitrides. The thermodynamic calculation of the equilibrium phases and the associated free formation energies have been calculated and presented in this work and show that MgO is formed first according to the Gibbs free energy followed by (Mg,Ca)S and carbonitrides and nitrides. SEM microscopy with EDS analysis confirmed the above-mentioned phases, in which it was discovered that MgO is present in nuclei, mostly embedded by sulphides. Nitrides were also found that contain Al, Mg and Si. MgO and the sulphides had a round shape, nitrides on the other hand had a rectangular shape. All the listed phases found in nuclei are solid after thermodynamic calculation before solidification.

From observations of the shapes and positions of phases in multiphase particles it can be concluded that MgO as a product of the Mg treatment process is a substrate for the growth of (Mg,Ca)S, we cannot state this for nitrides, because they were not in contact with other phases. From the presence of the above-mentioned phases and the absence of phases reported by other authors, it can be concluded that a nucleation mechanism is very complex and depends on the chemical composition of the melt, the melt treatment as Mg treatment and the inoculation process with different elements. The solidification process in terms of cooling rates also has an influence on the nucleation mechanism, which needs further investigation.

Acknowledgement

The authors acknowledge the financial support from the state budget by the Slovenian Research Agency (Programme Nos. P2-0132).

6 REFERENCES

[1] V. Nayyar, J. Kaminski, A. Kinnander, L. Nyborg: An Experimental Investigation of Machinability of Graphitic Cast Iron Grades. Flake, Compacted and Spheroidal Graphite Iron in Continuous Machining Operations, ed. by Proc. of the 5th CIRP Conference on High Performance Cutting, Zurich, 2012, 488–493, doi:10.1016/j.procir.2012.04.087

[2] S. Spaič, Fizikalna metalurgija: Binarni sistemi, Metalografija zlitin (Physical Metallurgy: Binary Systems, Metallography of Alloys), Faculty of Natural Sciences and Engineering, Department of Materials and Metallurgy, Ljubljana 2000, 350–352

[3] J. R. Brown, Foseco Ferrous Foundrymen's Handbook, Butterworth Heinemann, Oxford 2000

[4] C. Pelhan, S. Spaič, S. Malovrh, B. Urnaut, The effect of inoculants on hardness and machinability of grey cast iron with flake graphite, Livarski vestnik, 32 (**1985**) 2, 33–45

[5] V. Uršič, I. Surina, S. Semenič, M. P. Tonkovič: Development and usability of domestic complex inoculants for grey cast iron with flake graphite, 45. Symposium on Metallurgy and Metallic Materials, Portorož, 1995, 137–140

[6] T. Skaland, Nucleation Mechanisms in Ductile Iron, Proc. of the AFS Cast Iron Inoculation Conference, , Schaumburg, 2005, 1–30

[7] G. Alonso, P. Larranñaga, E. De la Fuente, D. M. Stefanescu, A. Natxiondo, R. Suarez, Kinetics of nucleation and growth of graphite at different stages of solidification for spheroidal graphite iron, Int. J. Metalcast, 11 (**2017**) 1, doi:10.1007/s40962-016-0094-7

[8] D. M. Stefanescu, G. Alonso, P. Larrañaga, R. Suarez, On the stable eutectic solidification of iron-carbon-silicon alloys, Acta Mater., 103 (**2016**) 15, doi:10.1016/j.actamat.2015.09.043

[9] Y. Igarashi, S. Okada, Observation and analysis of the nucleus of spheroidal graphite inmagnesium-treated ductile iron, Int. J. Cast. Met. Res., 11 (**1998**) 2, doi:10.1080/13640461.1998.11819261

[10] H. Nakae, Y. Igarashi, Influence of Sulfur on Heterogeneous Nucleus of Spheroidal Graphite, Mater. Trans., 43 (**2002**) 11, 2826–2831, doi:10.2320/matertrans.43.2826

[11] T. Skaland, Ø. Grong, T. Grong, A Model for the Graphite Formation in Ductile Cast Iron: Part I. Inoculation Mechanisms, Metall. Trans. A, 24 (**1993**) 10, doi:10.1007/BF02648605

[12] D. M. Stefanescu, G. Alonso, P. Larra, E. De la Fuente, R. Suarez, Reexamination of crystal growth theory of graphite in iron-carbon alloys, Acta Mater., 139 (**2017**) 15, doi:10.1016/j.actamat.2017.08.004

[13] M. Petrič, P. Mrvar, S. Kastelic, Electrical Resistivity Measurements During Solidification of Grey Cast Iron, The 11th Inter. Symp. on the Science and processing of Cast iron, Jönköping, 2017, 34–135

[14] P. Mrvar, M. Petrič, Insitu Measurement of Electrical Resistivity, Dilatometry and Thermal Analysis of Cast Iron, TMS 2018 147th Annual Meeting & Exhibition Supplemental Proceedings, Phoenix, 2018, 931–942

[15] A. Kaminska, E. Basinska, Z. Stefansi, M. Angrecki, Comparison of the Oxygen, Nitrogen and Hydrogen Content in Ductile Iron Castings and Their Effect on Microstructure and Mechanical Properties, Trans. Res. Foundry Inst., 57 (**2017**) 4, doi:10.7356/iod.2017.38

[16] F. Mampaey, D. Habets, F. Seutens, The Use of Oxygen Activity Measurement to Determine Optimal Properties of Ductile Iron During Production, Int. Foundry Res., 60 (**2008**) 1, 2–19